



Proceedings of the Sixth International Conference on
Railway Technology: Research, Development and Maintenance
Edited by: J. Pombo
Civil-Comp Conferences, Volume 7, Paper 6.9
Civil-Comp Press, Edinburgh, United Kingdom, 2024
ISSN: 2753-3239, doi: 10.4203/cc.7.6.9
©Civil-Comp Ltd, Edinburgh, UK, 2024

Research on Dynamic Performance of No.18 Turnout of Passenger Dedicated Line at 400 km/h

B. Hou¹, Y. Zhu¹, D. Wang¹ and J. Pombo^{2,3}

¹School of Civil Engineering, Beijing Jiaotong University
Beijing, China

²Institute of Railway Research, School of Computing and Engineering,
University of Huddersfield
Huddersfield, UK

³IDMEC, Instituto Superior Técnico, Universidade de Lisboa
Lisboa, Portugal

Abstract

Currently, among the high-speed turnouts laid in China, the self-developed passenger dedicated line series has laid 8000 groups, accounting for more than 60 %. The research and development of high-speed EMUs with a speed of 400 km / h has been fully carried out, but there is no high-speed turnout suitable for this speed standard. Addressing the gap, this paper focuses on No. 18 turnout of passenger dedicated line and establishes a rigid-flexible coupling dynamics model for the vehicle-turnout system to study the dynamic performance of the train crossing the turnout under operation conditions of 400 km/h. The dynamic performance of the turnout system is evaluated from wheel-rail interaction, safety indicators and stability indicators. Significant fluctuations are observed in wheel-rail interaction at the switch area and frog area during the transition over the switch rails and point rails, but all remain within safe limits. The trend in safety indicators is similar to that of vertical and lateral wheel-rail forces. All stability indicators meet the requirements. As train speeds increase, the vertical forces during straight and lateral crossing of the turnout noticeably intensify.

Keywords: high-speed railway, turnout, dynamic response, rigid-flexible coupling, wheel-rail interaction, contrastive analysis.

1 Introduction

High-speed turnout is an indispensable key equipment in high-speed railway, which can make the train transfer from one track to another or cross another track, providing flexibility for line operation [1]. However, the turnout structure is complex and the state is changeable. In particular, the structural irregularity is large and the stiffness distribution is uneven. The dynamic interaction of the train wheel passing through is much more complicated than that on the straight or curved track in the general interval, which will cause huge impact and vibration. When the train is running at high speed, this dynamic interaction is more intense. In order to reduce the impact effect between wheel and rail, the speed of the turnout area is set lower in the past. However, with the continuous development of high-speed railways, the demand for increasing the speed of trains passing through turnouts is becoming more and more urgent.

Many scholars have studied the dynamic characteristics between vehicles and tracks in turnout sections. Ren, Chen and Wang et al. [2-4] established a vehicle-turnout coupling model, and studied the influence of different reduction values of switch rail and nose rail on the dynamic response. BurgeLMAN N and Johansson A et al. [5] did not consider the dynamic vibration response of the basic rail of the sharp rail, and regarded the constraint of the basic rail of the sharp rail as rigid, and studied the fatigue characteristics and damage of the wheel-rail. Xin et al. [6] established a three-dimensional dynamic finite element model of wheel-turnout coupling by using the measured wheel, wing rail and frog geometry, and studied the dynamic response characteristics of the wheel-rail in the frog center when the train passes through the frog area under different parameter conditions. Sadeghi [7] successfully constructed a mathematical model of vehicle-turnout coupling, verified and analyzed the sensitivity of the model, and studied the influence of turnout geometric parameters such as curve radius, turnout angle and gauge on operation safety at different train speeds. Xu [8] studied the wheel-rail dynamic interaction when the turnout appeared to climb, and analyzed the influence of wheel-rail contact angle and friction coefficient on the performance of derailment behavior in turnout area. Hu [9] used the method of time-frequency slice and numerical simulation to decompose the vibration signal to extract the extraction of turnout impact force and the identification of position difference. Hamarat [10] first emphasized the dynamic phenomenon of turnout system considering various materials. Through the multi-body simulation of vehicle-turnout dynamic interaction, the influencing factors such as train-turnout dynamic response, load redistribution, dynamic impact factor and wheel-rail contact force are deeply analyzed. Wang et al. [11] optimized the rail profile to reduce the rolling circle radius difference (RRD), and proposed a rail profile optimization method to improve the operation stability of high-speed railway turnout vehicles, which has high work efficiency. Based on the vehicle-turnout coupling model, Chang et al. [12] proposed a turnout switch rail reduction optimization model based on multi-island genetic algorithm to minimize the dynamic response of the train passing through the turnout directly. Cao et al. [13] proposed a method to optimize the turnout geometry by controlling the transition region of the vehicle load on the rail surface, which can improve the stability of the vehicle passing through the turnout. Drozdzeil

et al. [14] studied the dynamic interaction between railway vehicles and turnouts and standard turnout intersections and the influence of wheel-rail force and vehicle motion and parameter deviation under standard track geometric parameters.

Currently, among the high-speed turnouts laid in China, the self-developed passenger dedicated line series has laid 8000 groups, accounting for more than 60 %. Further increasing operational speeds is a key direction for the advancement of high-speed railway technologies in China. The research and development of high-speed EMUs with a speed of 400 km / h has been fully carried out, but there is no high-speed turnout suitable for this speed standard. Addressing the gap, this paper focuses on No. 18 turnout of passenger dedicated line and establishes a rigid-flexible coupling dynamics model for the vehicle-turnout system to study the dynamic performance of the train crossing the turnout under operation conditions of 400 km/h.

2 Vehicle-Turnout System Model

The vehicle-turnout system model is made up of the vehicle and turnout model, which is coupled by the wheel/rail interaction. This model is used to calculate the dynamic responses in the vehicle-turnout system.

2.1 Vehicle Model

The calculation model of the vehicle is established as a space multirigid body model by SIMPACK, including modelling of the car body, suspension elements, bogies, and wheelsets. The vehicle model in this work is established on the basis of the parameters of the type of CRH380B vehicle (referred to Table 1). As shown in Figure 1, according to the structural type and vibration characteristics of the vehicle, the surge, sway, heave, roll, pitch, and yaw of the car body, the bogie, and the wheelsets are considered respectively, and the rest of the motions are considered to be rigidly connected to the body.

Parameter	Value	Unit
The mass of car body	38054	kg
The rolling moment of inertia of car body	98300	kg m ²
The nodding moment of inertia of car body	1773000	kg m ²
The yawing moment of inertia of car body	1744000	kg m ²
The mass of bogie	2271	kg
The rolling moment of inertia of bogie	1876	kg m ²
The nodding moment of inertia of bogie	1135	kg m ²
The yawing moment of inertia of bogie	2763	kg m ²
The mass of wheel set	1516	kg
The rolling moment of inertia of wheel set	1095	kg m ²

The nodding moment of inertia of wheel set	120	kg m ²
The yawing moment of inertia of wheel set	1101	kg m ²
Longitudinal/lateral/vertical stiffness of primary suspension	920/920/886	kN/m
Vertical damping of primary suspension	10.4	kN·s/m
Longitudinal/lateral/vertical stiffness of secondary suspension	124/124/182	kN/m
Vertical damping of secondary suspension	10.4	kN·s/m

Table 1: Vehicle parameters.

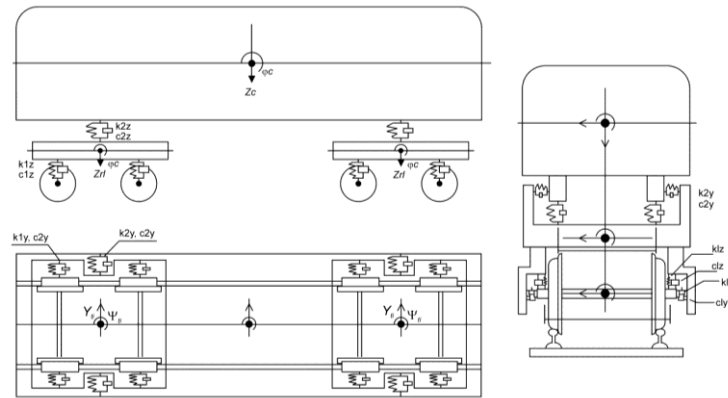


Figure 1: Vehicle model.

2.2 Turnout Model

The studied turnout is a standard one (right turn) with a curve radius of 1,100 m and a crossing angle of 1:18. In this paper, not only the flexibility of the turnout structure is considered in the modelling of the turnout, but also the spatial variable cross-section characteristics of the rails and many nonlinear mechanical factors in the turnout area are considered in detail by ANSYS (Figure 2). On this basis, a complete turnout model including the switch, closure, and crossing panels is established, which can completely reflect the structural characteristics of the turnout in each area. Through the SIMPACK module, the ANSYS sub-model is subjected to sub-structural and modal analyses, and then the results are imported into SIMPACK and combined with the SIMPACK sub-module to form a flexible turnout module.

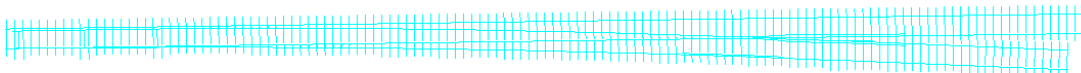


Figure 2: Overall schematic diagram of No. 18 turnout model (ANSYS module).

2.3 Wheel-Rail Contact

The coupling of the vehicle and turnout models is implemented by the wheel-rail interaction. When calculating the wheel-rail contact force, the normal contact force is calculated according to the Hertzian contact model, and the tangential creep-slip force is calculated according to the FASTSIM algorithm. Considering the case of multi-point contact in the turnout area, it is possible to calculate the multi-point contact of the wheels with multiple strands of rail in the switch and crossing panels of the turnout. Figure 3 shows a schematic diagram of the multi-point contact between wheels and rails in the switch panel.

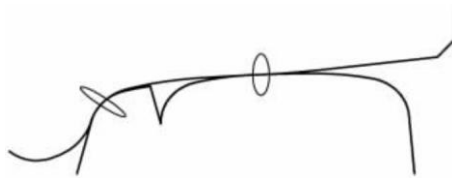


Figure 3: Multi-point contact at turnout zone.

3 Dynamic Interactions of Vehicle and Turnout

3.1 Speed of 400 km/h

When a 400 km/h locomotive group crosses the turnout in the straight direction, the lateral force of the first wheel which is the first to be impacted on both sides of the wheel-rail droop varies with the mileage of the turnout area as shown in Figure 4 and Figure 5.

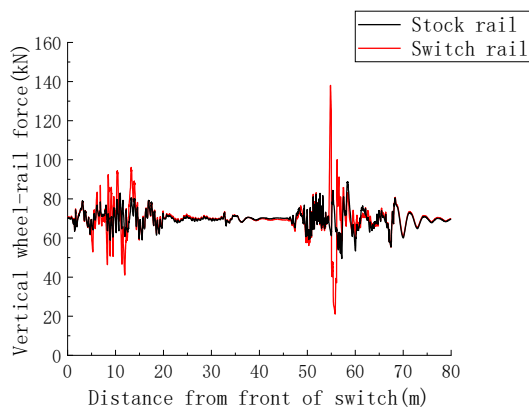


Figure 4: Vertical wheel-rail force of the first wheelset.

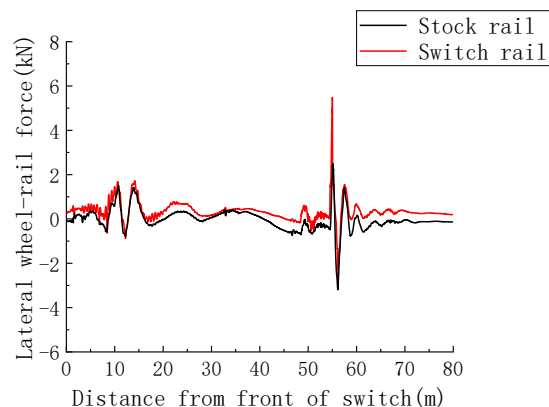


Figure 5: Lateral wheel-rail force of the first wheelset.

When the train is travelling on the turnout straight stock, the dynamic interaction between the wheel and rail is affected by the unevenness and rigidity of the turnout structure, compared with the straight basic rail side, the straight to the mile rail side in the rutters and rutted forks have larger wheel load fluctuations, and the rutted forks have the most prominent position of the heart rail.

When the train passes through the switch panel, the basic rail and the tip rail are close to each other, and the wheel load gradually completes the transition between the two rails, during which the phenomenon of wheel-rail multi-point contact occurs, and the impact of wheel-rail interaction becomes larger, and the vertical force of the wheel-rail on the side of the straight to the inside rail fluctuates from about 70kN to nearly 100kN, and at the same time, the transverse force of the wheel-rail increases from 0.12kN to about 2kN. After passing through the rutters, the wheel-rail fluctuation gradually decreases.

Train travelling to the crossing panel, crossing part of the composition of the complex, the wheel rolling through the impact of the fork centre produces a violent impact, resulting in a peak wheel-rail interaction force. The maximum wheel-rail vertical force is 138.03kN, not exceeding the limit value of 170kN, there is still a large margin of safety. This type of fork rutting fork part of the movable centre rail structure, wheel-rail transverse impact is relatively small, wheel-rail transverse force maximum 5.44kN, far less than the limit value of 56kN.

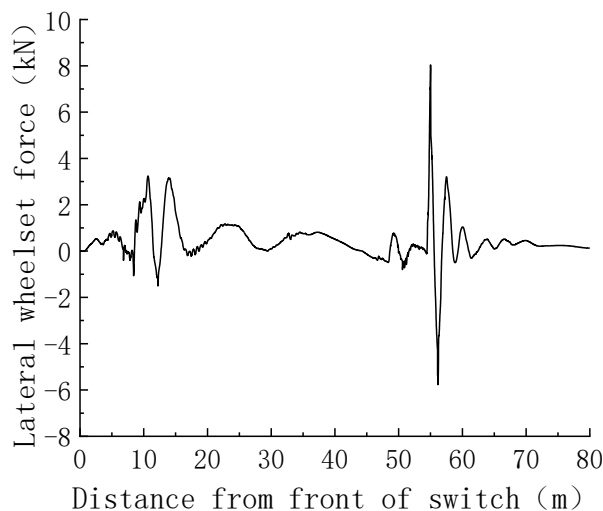


Figure 6: Lateral force of the first wheelset.

The fluctuation distribution of the lateral force of the first wheelset along the mileage is shown in Figure 6, and the change trend is roughly the same as that of the wheel-rail transverse force. When the train passes through the turnout, in the rutters part, the maximum value of the axle transverse force is 3.24kN, which is caused by the larger transverse force generated when the wheel hits the sharp rail, and in the rutted fork part of the turnout centre area the axle transverse force generates a peak value of 8.03kN, which does not exceed the limit value of the axle transverse force of 61.7kN.

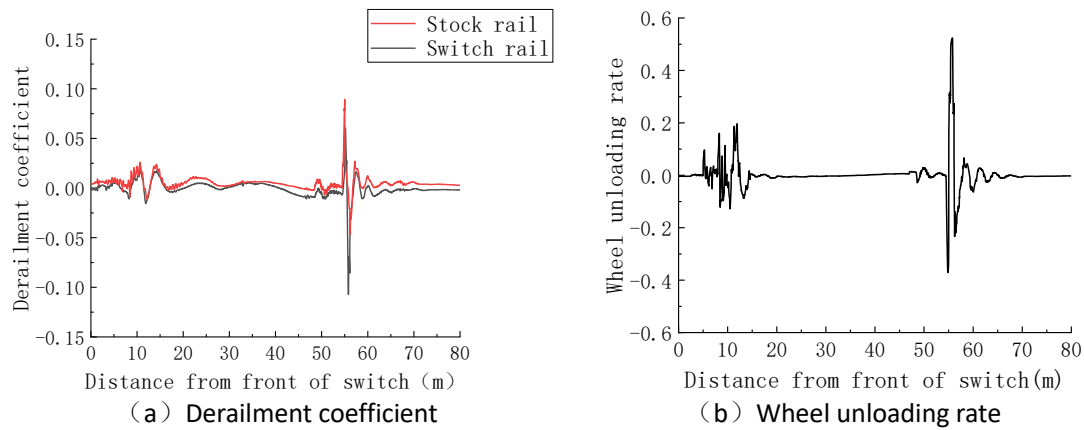


Figure 7: Safety indicators.

Train straight through the No. 18 turnout, safety indicators derailment coefficient and wheel unloading rate shown in Figure 7. Derailment coefficient and wheel-rail lateral force has a high correlation, its change rule is more consistent, when the train through the rutted fork area of the heart of the rail part of the maximum value of 0.09, far less than the limit value of 0.8; Wheel unloading rate and the wheel-rail vertical force with the mileage distribution of the turnout area with the similar pattern of change, the maximum also appeared in the rutting part of the fork, the maximum value of 0.52, located in the safety limit of 0.8 within, there is a certain amount of leeway. When the speed is 400km/h, the safety of train operation meets the requirements.

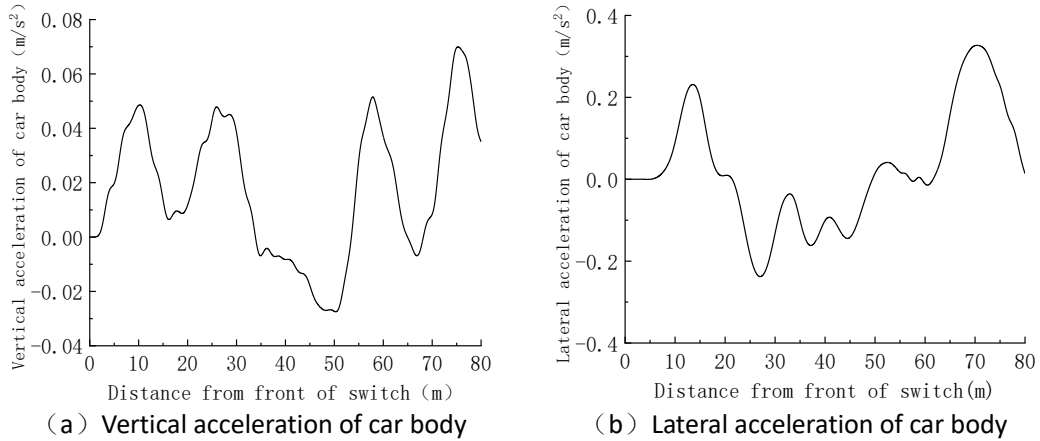


Figure 8: Stability indicators.

When the train passes the No. 18 turnout in the straight direction, the change curve of the vertical and lateral vibration acceleration of the car body is shown in Figure 8. It can be seen that the complex structural changes of the turnout have less influence on the vibration acceleration of the car body, and the maximum values of the vertical and transverse acceleration of the car body are 0.07m/s^2 and 0.23m/s^2 , respectively, which indicates that the train has good smoothness of operation when passing through the turnout in the straight direction.

3.2 Different Driving Speeds

Based on the established vehicle-turnout coupling dynamics model, the dynamics response of a moving train set passing through a turnout in the straight direction at the speeds of 350km/h, 375km/h, 400km/h, 425km/h and 450km/h is calculated, and the results of each dynamics index are as follows:

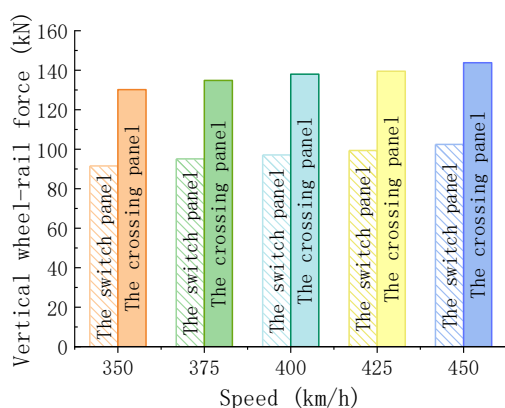


Figure 9: Comparison of vertical wheel-rail forces at different driving speeds.

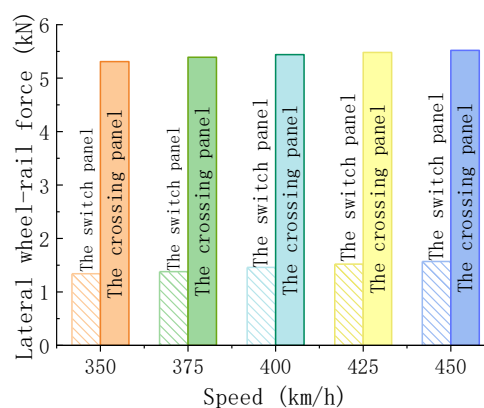


Figure: 10 Comparison of lateral wheel-rail forces at different driving speeds.

The results of the variation of the vertical transverse force on the wheel-rail at the straight-in rail side of the first wheel when the train passes the No. 18 turnout in the straight direction at different speeds are shown in Figure 9 and Figure 10. With the gradual increase of the speed of crossing the turnout in the straight direction, the impact of the wheel-rail at the centre rail of the pointed rail intensifies, and the peak vertical force on the wheel-rail on the straight-in-rail side of the rutting device area and rutting fork area both increase sharply. Under different speeds, the maximum wheel-rail vertical force in the rutters area is 91.54kN, 95.12kN, 97.10, 99.36, 102.43, with a maximum change rate of 11.89%, and the maximum wheel-rail vertical force in the rutters area is 130.17kN, 134.84kN, 138.03kN, 139.49kN, 143.82kN, with a maximum change rate of 10.49%. The maximum change rate is 10.49%, and the vertical force increase of the wheel-rail in the rutters and rutting fork area is close. When the train running speed is increased to 450km/h, the peak value of the wheel-rail vertical force meets the limit requirements, and there is a certain safety margin.

After the speed increase of straight overfork, relative to the change of wheel rail vertical force, the increase of wheel rail transverse force is small, and the maximum value of wheel rail transverse force on the side of straight overfork at different speeds, the maximum value of the rutters area is 1.47kN, 1.51kN, 1.59kN, 1.65kN, 1.70kN, and that of rutted fork area is 5.31kN, 5.39kN, 5.44kN, 5.48kN, respectively, 5.52kN.

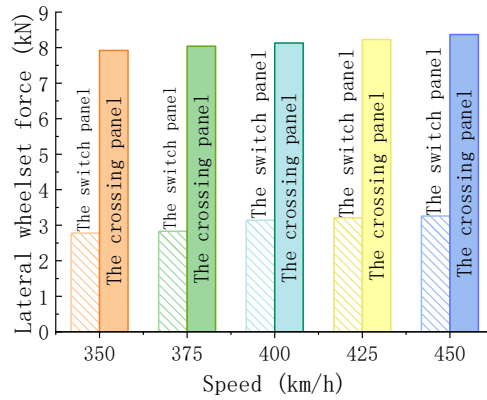
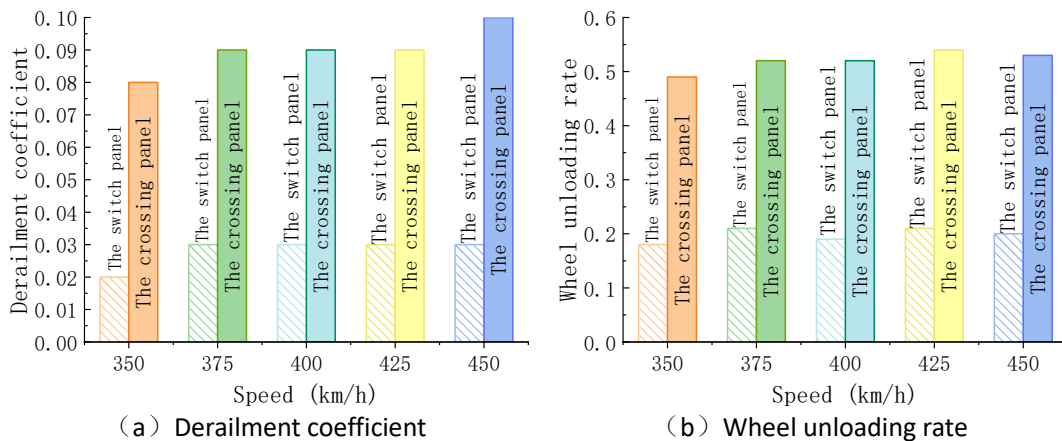


Figure 11: Comparison of lateral wheelset forces at different driving speeds.

As shown in Figure 11, the maximum values of wheel-axle transverse force in the rutted fork area are 7.92kN, 8.04kN, 8.13kN, 8.23kN, 8.37kN under each straight-forward crossing speed, which are similar to the change of wheel-rail transverse force. When crossing the turnout in the straight direction, with the increase of travelling speed, due to the special track structure in the turnout area, there is a wheel load transition at the tip rail and heart rail, which makes the interaction between the wheel and rail change significantly.



(a) Derailment coefficient (b) Wheel unloading rate
Figure 12: Comparison of safety indicators at different driving speeds.

The change of safety indexes when the train passes through the No. 18 turnout in the straight direction at different speeds is shown in Figure 12. The increase in operating speed has a small effect on the derailment coefficient. When the speed of 350 km/h is increased to 450 km/h, the maximum value of the derailment coefficient of the rutters area changes from 0.02 to 0.03, and the maximum value of the derailment coefficient of the rutted fork area changes from 0.08 to 0.10, which is still a large margin from the safety limit value of 0.8. When crossing the fork at high speed, the wheel load shedding rate is not obvious in relation to the change of speed, and the maximum value of wheel load shedding rate is 0.18, 0.21, 0.19, 0.21, 0.20 in the rutting device area under various speeds, and 0.49, 0.52, 0.52, 0.54, 0.53 in the rutting fork area, which do not appear to exceed the safety limit, and all of them satisfy the safety needs.

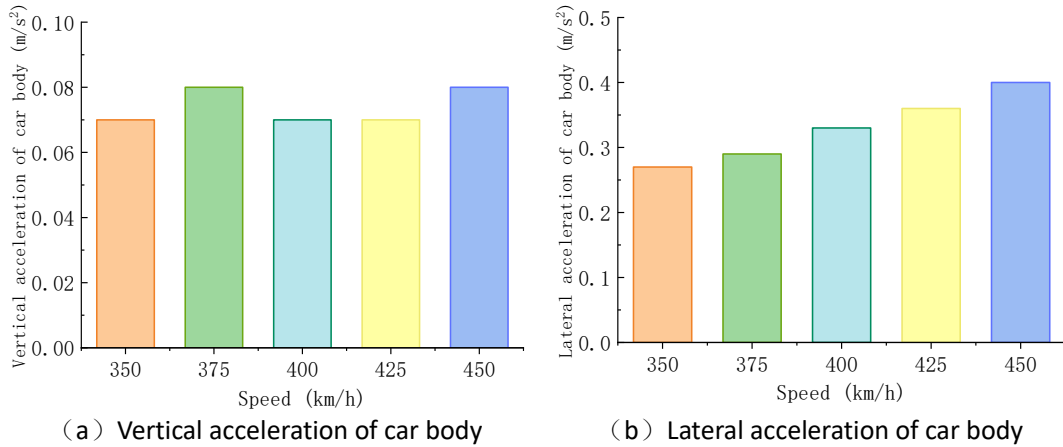


Figure 13: Comparison of stability indicators at different driving speeds.

The vertical and lateral acceleration changes of the car body when the train passes through the No. 18 turnout in the straight direction at different speeds are shown in Figure 13. As the suspension of the vehicle plays the role of damping and buffering, the vertical acceleration of the car body when passing through the turnout area at various speeds is small, and the fluctuation of the change is not big. The transverse acceleration of the car body increases with the train speed and the trend is obvious, and the maximum value of the transverse acceleration of the car body under each speed is $0.27m/s^2$, $0.29m/s^2$, $0.33m/s^2$, $0.36m/s^2$, $0.40m/s^2$, respectively, which all have good smoothness of travelling.

4 Conclusions and Contributions

This paper establishes a vehicle - turnout system dynamics analysis model, from the wheel-rail interaction, safety indicators, stability indicators of the three aspects of the study of the dynamic performance of 400km/h under the operating strip of the passenger dedicated line No. 18 turnout straight over the turnout, and the impact of changes in the speed of the train to be analysed.

When the train passes through the No. 18 single-open switch of the passenger dedicated line at a speed of 400km/h in a straight direction, the wheel-rail interaction in the rutting device area and rutting fork area of the tip rail heart rail wheel load transition are all fluctuating greatly. Rutting fork area heart rail position is the most intense, here produce wheel rail vertical force peak 138.03kN, wheel rail transverse force peak 5.48kN and wheel axle transverse force peak 61.7kN. safety indicators change trend is similar to the wheel rail vertical and transverse force, derailment coefficient and the maximum value of the wheel load reduction rate of 0.23 and 0.63, respectively, less than the limit value to meet the safety requirements. The maximum values of vertical and lateral vibration acceleration of the car body are $0.07m/s^2$ and $0.23m/s^2$ respectively, which indicates that the 400km/h high-speed train has good smoothness of operation when it crosses the turnout in the straight direction.

With the increase of train speed, the vertical force of wheel-rail when crossing the turnout in the straight direction increases obviously, and the peak value of vertical

force corresponding to the maximum speed of 450km/h is 143.82kN, and there is a certain safety margin from the limit value of 170kN. The wheel-rail interaction force in the transverse direction increases less when crossing the fork in the straight direction. There is no obvious correlation between the change of vertical acceleration and travelling speed, and the trend of the transverse acceleration of the car body is obvious when the train speed is increased, and the peak value of the whole speed range is smaller than the limit value of the stability indicators.

Acknowledgements

This research is supported by China National Railway Group Co., Ltd (P2021G053).

References

- [1] Wang P. Design of High-Speed Railway Turnouts: Theory and Applications [J]. 2015: 443–450.
- [2] Chen R, Wang P, Quan S X. Dynamic performance of vehicle-turnout-bridge coupling system in high-speed railway[J]. Applied Mechanics Materials, 2011, 50: 654-658.
- [3] Ren Z, Sun S, Xie G. A method to determine the two-point contact zone and transfer of wheel–rail forces in a turnout[J]. Vehicle system dynamics, 2010, 48(10): 1115-1133.
- [4] Wang S, Si D, Wang M, et al. Influence of value reduced for switch rail of high speed railway on riding quality[J]. China Railway Science, 2014, 35: 28-33.
- [5] Burgelman N, Li Z, Dollevoet R. A new rolling contact method applied to conformal contact and the train–turnout interaction[J]. Wear, 2014, 321: 94-105.
- [6] Xin L, Markine V, Shevtsov I. Numerical analysis of the dynamic interaction between wheel set and turnout crossing using the explicit finite element method[J]. Vehicle System Dynamics, 2016, 54(3): 301-327.
- [7] Sadeghi J, Masnabadi A, Mazraeh A. Correlations among railway turnout geometry, safety and speeds[C]. Proceedings of the Institution of Civil Engineers-Transport, 2016: 219-229.
- [8] Xu J, Wang J, Wang P, et al. Study on the derailment behaviour of a railway wheelset with solid axles in a railway turnout[J]. Vehicle System Dynamics, 2019.
- [9] Hu H, Qin H, Shi J, et al. Identification of high-speed railway turnout generated vibrations based on time–frequency slice and mutual correlation of vibration responses from axle box[J]. Measurement, 2023, 221: 113458.
- [10] Hamarat M, Kaewunruen S, Papaalias M, et al. New insights from multibody dynamic analyses of a turnout system under impact loads[J]. Applied Sciences, 2019, 9(19): 4080.
- [11] Wang P, Ma X, Wang J, et al. Optimization of rail profiles to improve vehicle running stability in switch panel of high-speed railway turnouts[J]. Mathematical Problems in Engineering, 2017, 2017.
- [12] Chang W, Cai X, Wang P, et al. Optimizing reduced values of switch rails during the service time of high-speed railway turnouts[J]. Journal of Transportation Engineering, Part A: Sys-tems, 2022, 148(6): 04022031.

- [13] Cao Y, Zhao W, Lin Y, et al. Dynamic optimization of the rail-crown geometry in the rigid frog area by controlling the position of the wheel-load transition[J]. Proceedings of the Institution of Mechanical Engineers, Part F: Journal of Rail and Rapid Transit, 2020, 234(9): 1017-1028.
- [14] Drożdżiel J, Sowiński B, Groll W: The effect of railway vehicle-track system geometric deviations on its dynamics in the turnout zone, The Dynamics of Vehicles on Roads and on Tracks: CRC Press, 2021: 641-652.